

# Specific Harmonic Power Suppression of Direct-Power-Controlled Current-Source PWM Rectifier

Toshihiko Noguchi <sup>\*</sup>, *IEEE Senior Member*, and Kohji Sano <sup>\*</sup>

<sup>\*</sup> Nagaoka University of Technology  
Address: 1603-1 Kamitomioka, Nagaoka, Niigata 940-2188, Japan  
Phone: +81-258-47-9510, Fax: +81-258-47-9500  
e-mail: tnoguchi@vos.nagaokaut.ac.jp

**Abstract**— This paper focuses on specific harmonic active power suppression of a direct-power-controlled (DPC) PWM current-source rectifier (CSR) in order to achieve low distortion of the input line currents. Total input power factor of the DPC-based PWMCSR becomes worse as the load gets lower due to the low-order harmonics in the line currents, especially the fifth and the seventh. Since the dominant low-order harmonic currents cause an oscillation in the active power at frequency of sixth, suppression of the sixth-order harmonic active power is essential to improve the total power factor particularly in the low-load range. The paper describes a theoretical aspect and a suppression technique of the harmonic active power, followed by basic configuration and operation of the DPC-based PWMCSR. Effectiveness of the proposed technique is confirmed through computer simulations and experimental tests, using a 2-kW prototype. As a result, the total harmonic distortion of the line currents is effectively reduced by 10 %, which results in approximately 20-% improvement of the total input power factor at a 350-W load condition

**Index Terms**— current-source PWM rectifier, direct power control, relay control, instantaneous power, and harmonic power suppression.

## I. INTRODUCTION

In general, PWM rectifiers are extensively used as an AC/DC power converter in order to improve the total input power factor. There are two classes of the PWM rectifiers, i.e., a voltage-source rectifier and a current-source rectifier. The two rectifiers are dual with each other from the viewpoint of the circuit topology, and the former has been intensively investigated and widely been applied to various industry applications, compared with the latter. In both cases, conventional control strategies of the PWM rectifiers achieve a unity power factor operation by forcing the input line currents in phase with the power-source voltages. Therefore, most of the conventional systems have a current minor control loop with a rotational coordinate transformation like AC motor drive systems. However, this approach has some drawbacks as pointed out below.

- (1) It inherently suffers from a slow response due to the current minor loop, especially due to PI regulators.
- (2) It is difficult to reduce its capacitive or inductive value in the DC-bus energy buffering devices.
- (3) Its control algorithm is inherently complicated due to the rotational coordinate transformation.
- (4) It requires a pulse width modulator to generate switching signals for the power devices.

- (5) In order to make the unity power factor operation possible, high-resolution in detecting relative phase of the power-source voltage is indispensable.
- (6) Under some conditions where waveform distortion and/or unbalance in the power-source occur, it requires additional circuits to cope with such cases.

The authors have been investigating a direct power control (DPC) strategy of various power converters to overcome the drawbacks mentioned above. The key of this strategy is a direct selection of optimum switching states to perform high-speed relay (bang-bang) control of the instantaneous active and reactive power of the converters. This eliminates the pulse width modulator and the PI regulators in the current minor loop, which leads to extremely quick response and high controllability of the power. By controlling the active power at a constant value and the reactive power to be zero, sinusoidal line currents in phase with the power-source voltages are resultantly obtained with neither the current minor loop nor the rotational coordinate transformation. Furthermore, the DPC system does not need any auxiliary compensator against the waveform distortion and/or the unbalance of the power-source, which is a unique feature of this approach.

However, the DPC still has some problems as follows:

- (1) Switching frequency of the converter varies as the load and/or operating condition change, which makes input filter design difficult.
- (2) Waveform distortion of the line currents apt to be worse in the low-load range.
- (3) The system performance is rather sensitive to delay time in the power feedback paths.

This paper discusses a compensation technique for the waveform distortion of the line currents in order to improve the total power factor in the low-load range, focusing on the DPC based PWM current-source rectifier (CSR). Through several computer simulations and experimental tests, the proposed technique is found to be effective to reduce the low-order harmonic currents and to improve the total input power factor without sacrificing inherent advantages of the DPC strategy.

## II. BASIC CONFIGURATION AND OPERATION

### A. System Configuration

Fig. 1 shows a schematic diagram of the DPC-based PWMCSR. As shown in the figure, relay (bang-bang) control of the instantaneous active power  $P$  and the

instantaneous reactive power  $Q$  is performed with use of their feedback values. Both of  $P$  and  $Q$  are calculated as expressed in the following equations:

$$\begin{bmatrix} v_\alpha \\ v_\beta \end{bmatrix} = \sqrt{\frac{2}{3}} \begin{bmatrix} 1 & -1/2 & -1/2 \\ 0 & \sqrt{3}/2 & -\sqrt{3}/2 \end{bmatrix} \begin{bmatrix} v_u \\ v_v \\ v_w \end{bmatrix}, \quad (1)$$

$$\begin{bmatrix} i_\alpha \\ i_\beta \end{bmatrix} = \sqrt{\frac{2}{3}} \begin{bmatrix} 1 & -1/2 & -1/2 \\ 0 & \sqrt{3}/2 & -\sqrt{3}/2 \end{bmatrix} \begin{bmatrix} i_u \\ i_v \\ i_w \end{bmatrix}, \text{ and} \quad (2)$$

$$\begin{bmatrix} P \\ Q \end{bmatrix} = \begin{bmatrix} v_\alpha & v_\beta \\ v_\beta & -v_\alpha \end{bmatrix} \begin{bmatrix} i_\alpha \\ i_\beta \end{bmatrix}. \quad (3)$$

As expressed in (3),  $P$  and  $Q$  can simply be calculated with an inner product and an outer product between the power-source voltage vector and the line current vector, respectively. On the other hand, the instantaneous active power command  $P^*$  is provided from a DC bus current control block, while the instantaneous reactive power command  $Q^*$  is directly given from the outside of the controller, according to the desired input total power factor. Zero command value for  $Q^*$  is normally given to the controller to achieve a unity input power factor operation. Control errors of the active and the reactive power, i.e.,  $\Delta P = P^* - P$  and  $\Delta Q = Q^* - Q$  are quantized with hysteresis comparators, of which outputs are digital signals  $S_p$  and  $S_q$ , respectively. In addition, a relative phase of the power-source voltage vector is quantized to six sectors  $\Theta_n$  by using several comparators as follows:

$$(n-2)\frac{\pi}{3} \leq \Theta_n < (n-1)\frac{\pi}{3} \quad \therefore n=1, 2, \dots, 6. \quad (4)$$

A combination of these quantized signals  $S_p$ ,  $S_q$  and  $\Theta_n$  is used to select uniquely the most appropriate switching state of the PWMCSR. In other words, every time the PWMCSR changes its switching state,  $S_p$ ,  $S_q$  and  $\Theta_n$  determine the next unique and optimum switching state to restrict  $\Delta P$  and  $\Delta Q$  within the corresponding hysteresis bands. In order to achieve this function, a switching state table is composed as shown in Fig. 2, of which contents are predefined so that both of the active and the reactive power follow their commands with small control errors. The uniquely selected switching state turns on or off every switching device in the PWMCSR. In the switching state table shown in Fig. 2, "P" stands for a state of  $S_{u,v,w}$  = "ON" and  $S_{x,y,z}$  = "OFF", "O" is a state of  $S_{u,v,w}$  = "OFF" and  $S_{x,y,z}$  = "OFF", "N" is a state of  $S_{u,v,w}$  = "OFF" and  $S_{x,y,z}$  = "ON", and "S" is a state of  $S_{u,v,w}$  = "ON" and  $S_{x,y,z}$  = "ON".

### B. Optimum Switching State Selection

Since the proposed DPC system is, in principle, based on relay control, it is absolutely significant to investigate relationship between the switching states of the PWMCSR and polarities of time derivatives of the active and reactive power  $dP/dt$  and  $dQ/dt$ . Their polarities correspond to the quantized signals  $S_p$  and  $S_q$ ; hence, the time derivatives of  $dP/dt$  and  $dQ/dt$  need be solved with respect to the switching states and the phase information

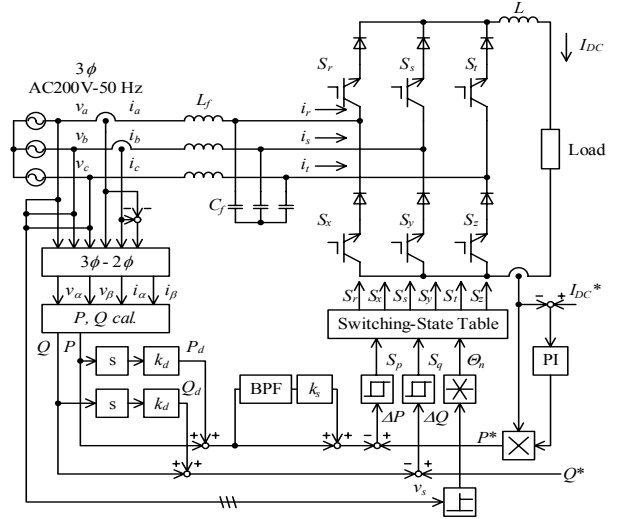


Fig. 1. System configuration of direct power control (DPC) based current-source PWM rectifier with specific harmonic power suppression

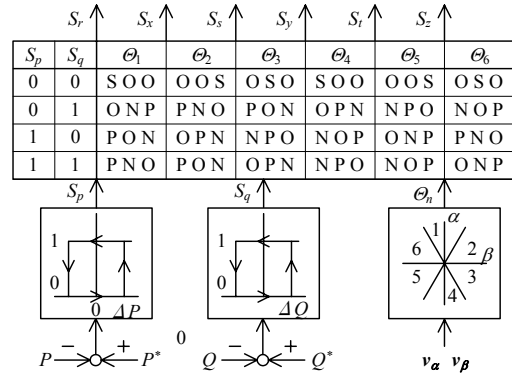


Fig. 2. Switching state table and power regulators.

of the power-source voltage vector in order to compose the switching state table appropriately.

From a mathematical model of the PWMCSR connected to the power grid shown in Fig. 3, the following current equation is established:

$$i_s + i_c = i_s + C_f \frac{dv_c}{dt} = i'_s, \quad (5)$$

where the power-source current vector is defined by

$$i_s = i_\alpha + j i_\beta = \sqrt{\frac{2}{3}} \left( i_u + i_v e^{j\frac{2\pi}{3}} + i_w e^{j\frac{4\pi}{3}} \right). \quad (6)$$

In the case of three-phase balanced power source, the above current is represented as a rotating vector with constant amplitude of  $I_{rms}$  expressed as

$$i_s = \sqrt{3} I_{rms} e^{j\omega t}. \quad (7)$$

In addition, the input current vector  $i'_s$  drawn by the PWMCSR is a function of the switching state as shown below, where  $I_{DC}$  is a DC bus current:

$$i'_s = \sqrt{\frac{2}{3}} I_{DC} \left( S_u + S_v e^{j\frac{2\pi}{3}} + S_w e^{j\frac{4\pi}{3}} \right). \quad (8)$$

On the other hand, the time derivatives of  $dP/dt$  and

$dQ/dt$  are derived from (3) and are approximated as indicated by the following equations because variation of the power-source current  $i_s$  can be regarded as negligibly small during switching intervals of the PWMCSR and capacitor voltage  $v_c$  is almost equal to the power-source voltage  $v_s$ :

$$\frac{dP}{dt} = i_s \cdot \frac{dv_s}{dt} + \frac{di_s}{dt} \cdot v_s \approx i_s \cdot \frac{dv_c}{dt}, \text{ and} \quad (9)$$

$$\frac{dQ}{dt} = i_s \times \frac{dv_s}{dt} + \frac{di_s}{dt} \times v_s \approx i_s \times \frac{dv_c}{dt}. \quad (10)$$

Substituting (5), (7) and (8) into the above equations,  $dP/dt$  and  $dQ/dt$  can be solved as follow:

$$\frac{dP}{dt} = -\frac{3I_{rms}^2}{C_f} + \frac{\sqrt{2}I_{rms}I_{DC}}{C_f} \left\{ (S_u - \frac{S_v}{2} - \frac{S_w}{2}) \cos \theta + \frac{\sqrt{3}}{2} (S_v - S_w) \sin \theta \right\}, \text{ and} \quad (11)$$

$$\frac{dQ}{dt} = \frac{\sqrt{2}I_{rms}I_{DC}}{C_f} \left\{ (S_u - \frac{S_v}{2} - \frac{S_w}{2}) \sin \theta - \frac{\sqrt{3}}{2} (S_v - S_w) \cos \theta \right\}, \quad (12)$$

where  $\theta$  is an argument of the power-source voltage vector. According to the polarities of  $dP/dt$  and  $dQ/dt$  solved as (11) and (12), one of the switching states of the PWMCSR can uniquely be determined to restrict the control errors  $\Delta P$  and  $\Delta Q$  within the hysteresis bands, which leads to determination of the whole contents of the optimum switching state table. Fig. 4 is an example of behaviors of the active and the reactive power when the power-source voltage vector is in the sector  $\theta_1$ , where the time derivatives  $dP/dt$  and  $dQ/dt$  are symbolized with tilted arrows.

### C. LC filter Resonance Suppression

The PWMCSR requires a LC filter at input terminals, which possibly causes current oscillation at the resonant frequency. Therefore, the DPC based PWMCSR has a compensator to damp the oscillation. A Laplace-transformed circuit equation of the PWMCSR with the LC filter shown in Fig. 3 can be described on a synchronous rotating reference frame as follows:

$$V_s = sL_f I_s + \frac{1}{sC_f} (I_s - I'_s). \quad (13)$$

Assuming that the power-source voltage and the input line current have a relative phase of  $\varphi$ , they can be expressed as

$$V_s = \sqrt{3}V_{rms}, \text{ and} \quad (14)$$

$$I' = \sqrt{3}I'_{rms}e^{-j\varphi}. \quad (15)$$

Substituting the above equations into (13), the power-source current  $I_s$  can be derived in an approximated expression as follows:

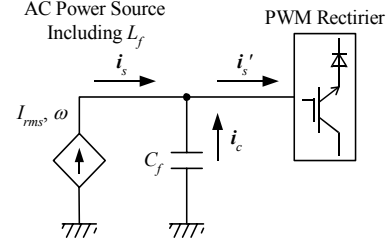


Fig. 3. Simplified mathematical model of PWMCSR.

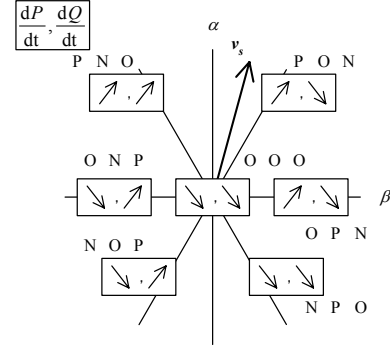


Fig. 4. Symbolized time derivatives of instantaneous active and reactive power in case of sector  $\theta_1$ .

$$I_s = \frac{\sqrt{3}V_{rms}C_f}{L_f C_f s^2 + 1} + \frac{\sqrt{3}I'_{rms}e^{-j\varphi}}{s(L_f C_f s^2 + 1)} \approx \frac{\sqrt{3}I'_{rms}e^{-j\varphi}}{s(L_f C_f s^2 + 1)}. \quad (16)$$

Applying an inverse Laplace-transform to (16), the following instantaneous apparent power  $S$  is calculated in the time domain:

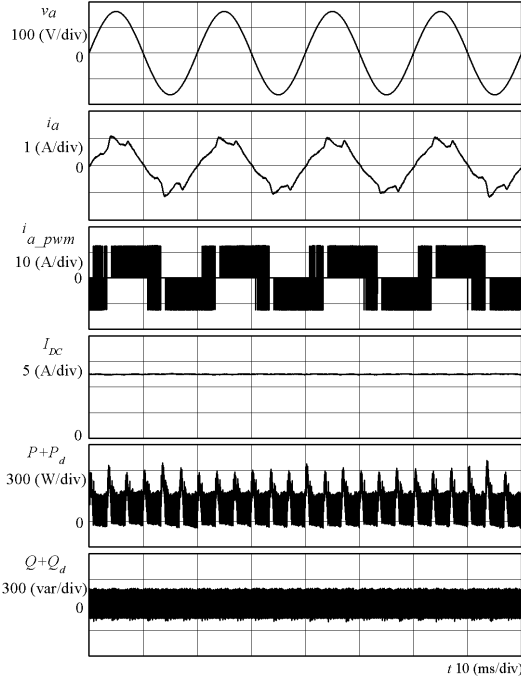
$$S = v_s \bar{i}_s = 3V_{rms}I'_{rms}e^{j\varphi} - 3V_{rms}I'_{rms}e^{j\varphi} \cos \frac{1}{\sqrt{L_f C_f}} t. \quad (17)$$

This equation shows that the first term corresponds to the fundamental frequency components of the active and the reactive power, while the second term is the resonant frequency components of them. Since the resonant components have no damping factor as indicated in (17), differential elements are added to the power feedback in order to damp the oscillation. Applying this feedback compensation converts the transfer function of the power-source current  $I_s$  to the following form:

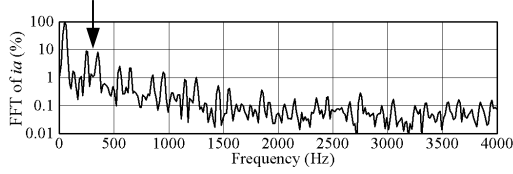
$$I_s \approx \frac{\sqrt{3}I'_{rms}e^{-j\varphi}}{s(L_f C_f s^2 + k_d s + 1)}. \quad (18)$$

Therefore,  $S$  can be damped by the derivative compensation elements, which are inserted in the feedback paths of the active and the reactive power. When the derivative gain is set at  $k_d = 2\sqrt{L_f C_f}$ , a critically damped response of  $S$  is achieved as

$$S = 3V_{rms}I'_{rms}e^{j\varphi} - 3V_{rms}I'_{rms}e^{j\varphi} \left( 1 + \frac{1}{\sqrt{L_f C_f}} t \right) e^{-\frac{1}{\sqrt{L_f C_f}} t}. \quad (19)$$



(a) Waveforms of power-source line-to-neutral voltage, input line current, PWM current, DC bus current, and active and reactive power.



(b) Frequency spectra of input line current.

Fig. 5. Operating waveforms without compensation at low load condition (simulation result).

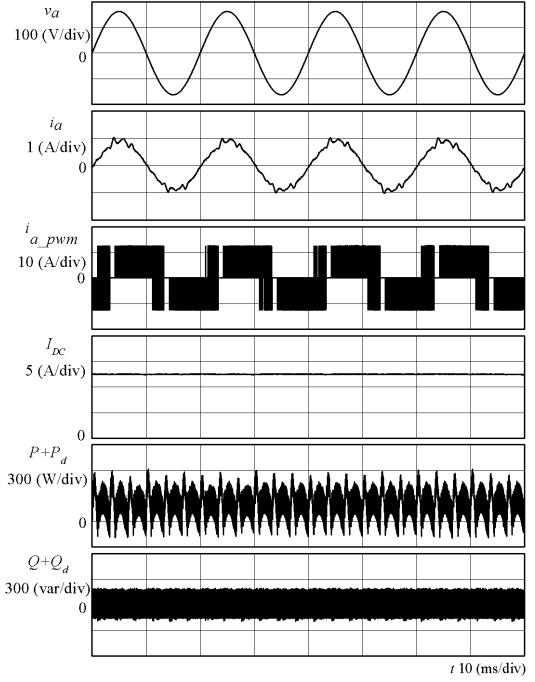
Table 1. Electric parameters of power circuit and test conditions.

Power source	AC 3 $\phi$ 200 V, 50 Hz
Input filter	$L_f = 2.7$ mH, $C_f = 40$ $\mu$ F
DC bus reactor	$L = 40$ mH
DC bus current command	$I_{DC}^* = 12.5$ A
Load power	220 W
Hysteresis bandwidth	300 W for $P$ , 300 var for $Q$
Central frequency of BPF	300 Hz (six times of 50 Hz)
Quality factor of BPF	20

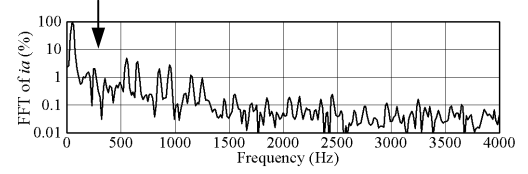
### III. SPECIFIC HARMONIC POWER SUPPRESSION

#### A. Requirements of Harmonic Power Suppression

As described earlier in this paper, although the control errors  $\Delta P$  and  $\Delta Q$  as well as the relative phase of the power source voltage vector  $\theta$  are quite roughly quantized, sinusoidal waveforms can resultantly be obtained in the input line currents without using a current minor loop, which is one of the significant features of the DPC based system. However, when the load power is in a relatively low range, low-order harmonics appear in the input line currents and detrimentally affects not only the total harmonic distortion (THD) level of the currents but also the total input power factor and the total efficiency. This phenomenon is particularly remarkable in as low-



(a) Waveforms of power-source line-to-neutral voltage, input line current, PWM current, DC bus current, and active and reactive power.



(b) Frequency spectra of input line current.

Fig. 6. Operating waveforms with sixth-order harmonic active power suppression at low load condition (simulation result).

load range as the hysteresis bandwidths  $\Delta P$  and  $\Delta Q$ . If the hysteresis bandwidths can be narrowed, this problem may be avoided. Due to the delay time in detection and calculation of the instantaneous active and reactive power, however, it is not impossible to restrict  $\Delta P$  and  $\Delta Q$  within the specified hysteresis bandwidths even though the bandwidths are reduced to nearly zero.

#### B. Theoretical Analysis of Harmonic Power

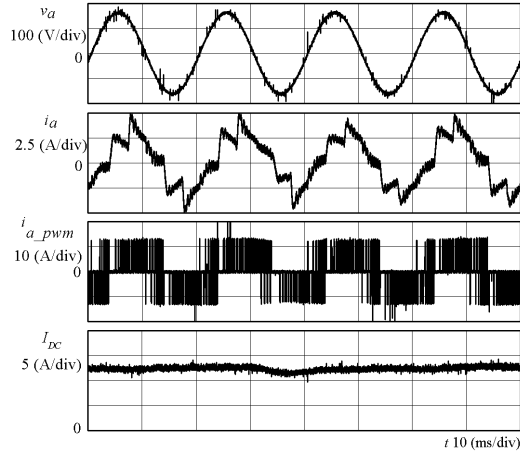
Assuming that the power-source supplies ideally balanced sinusoidal three-phase voltages to the DPC based PWMCSR, the power-source voltage vector can be expressed as

$$\mathbf{v}_s = \sqrt{3} V_{rms}^\omega e^{j\omega t}, \quad (20)$$

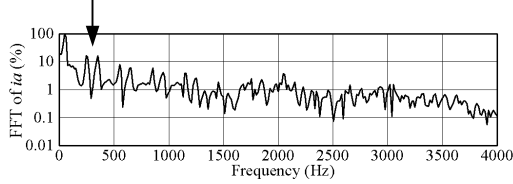
where a superscript of the root-mean-square value denotes an angular frequency  $\omega$  of the voltage vector. As described previously, the input line current vector has low-order harmonics; hence, its mathematical expression can be as follows:

$$\mathbf{i}_s = \sqrt{3} I_{rms}^\omega e^{j(\omega t - \varphi^\omega)} + \sqrt{3} I_{rms}^{5\omega} e^{-j(5\omega t - \varphi^{5\omega})} + \sqrt{3} I_{rms}^{7\omega} e^{j(7\omega t - \varphi^{7\omega})} + \dots \quad (21)$$

In this expression, the input line current vector is composed of a fundamental component and the harmonic



(a) Waveforms of power-source line-to-neutral voltage, input line current, PWM current, and DC bus current.



(b) Frequency spectra of input line current.

Fig. 7. Operating waveforms without compensation at low load condition (experimental result).

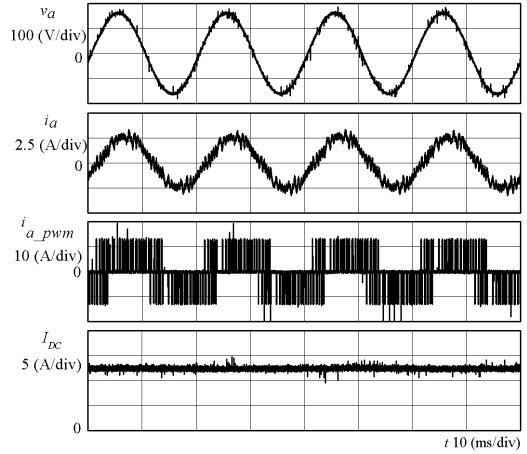
components except for multiples of the third-order harmonics because of a three-phase and three-line system. As can be seen in the second term of the above equation, the fifth-order harmonic component causes a negative sequence, whereas the fundamental and the seventh-order components constitute a positive sequence. Using these equations, the apparent power  $\mathcal{S}$  is derived as

$$\begin{aligned} \mathcal{S} = & 3V_{rms}^{\omega} I_{rms}^{\omega} e^{j\varphi} \\ & + 3V_{rms}^{\omega} I_{rms}^{5\omega} e^{j(6\omega t - \varphi^{5\omega})} + 3V_{rms}^{\omega} I_{rms}^{7\omega} e^{-j(6\omega t - \varphi^{7\omega})} + \dots \end{aligned} \quad (22)$$

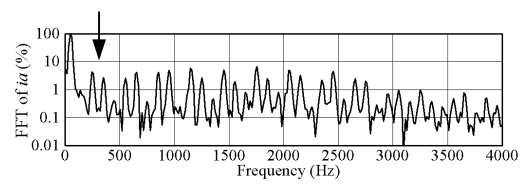
As indicated in (22), the apparent power  $\mathcal{S}$  has a static DC component brought by the fundamental components of the voltage and the current and the multiples of the sixth-order harmonic components, which result in the dominant oscillations of the active and the reactive power. Particularly, the real part of  $\mathcal{S}$ , i.e., the active power, is a major component of the sixth-order frequency. Therefore, suppression of the sixth-order harmonic active power is effective and essential to reduce the input line current distortion, especially low-order harmonic components such as the fifth and the seventh.

### C. Specific Harmonic Power Suppression

The fifth and the seventh harmonic distortion of the input line currents can simultaneously be suppressed by restricting specifically the sixth-order harmonic active power; thus minimization of the hysteresis bandwidth only for the sixth-order harmonic active power is required in the DPC system. In order to achieve this goal, a feedback signal of only the sixth-order harmonic active power is selectively magnified by extracting the sixth-



(a) Waveforms of power-source line-to-neutral voltage, input line current, PWM current, and DC bus current.



(b) Frequency spectra of input line current.

Fig. 8. Operating waveforms with sixth-order harmonic active power suppression at low load condition (experimental result).

order harmonic component with a band-pass filter (BPF) as shown in Fig 1. The central frequency of the BPF is adjusted at a frequency of the sixth, and the quality factor is tuned to have an appropriate damping characteristic. The proposed technique can effectively diminish the fifth and the seventh harmonic currents at the same time without sacrificing inherent simple configuration of the DPC based PWMCSR.

## IV. COMPUTER SIMULATION RESULTS

In order to examine basic operation characteristics of the proposed technique, some computer simulations were conducted with PSIM, where electric parameters of the power circuit and test conditions are listed in Table 1.

Fig. 5 shows operating waveforms and frequency spectra of the input line current at as low load as 220 W with no compensation. As shown in Fig. 5 (a), a large waveform distortion can be seen in the line current due to the low-order harmonics caused by active power deviation out of the specified hysteresis band. The ripples of the active power appear six times per cycle, i.e., 300 Hz, whereas the reactive power is properly restricted within the predetermined hysteresis band. This sixth-order harmonic active power brings the fifth and the seventh harmonic currents as indicated by a downward arrow in Fig. 5 (b), which are more than 10 % of the fundamental component. On the other hand, Fig. 6 depicts operating characteristics at 220-W load power where the proposed compensation technique is applied to the system. As shown in the line current waveform, undesirable large ripples are effectively reduced around peaks of the current, resulting in the sinusoidal waveform. This effect can be confirmed in the frequency spectra of

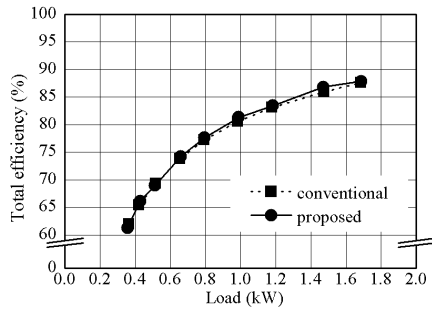


Fig. 9. Total efficiency characteristics with/without sixth-order harmonic active power suppression (experimental result).

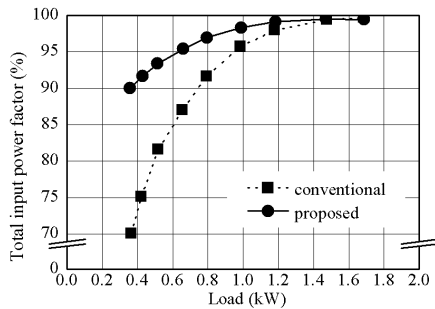


Fig. 10. Total input power factor characteristics with/without sixth-order harmonic active power suppression (experimental result).

the line currents shown in Fig. 6 (b), where the fifth and the seventh harmonics are diminished down to approximately 1 %.

## V. EXPERIMENTAL RESULTS

The proposed compensation technique was examined with a 2-kW prototype that is composed of analog and digital mixed signal hardware. The prototype has the similar specifications and parameters as used in the computer simulations.

Fig. 7 shows an experimental result at low-load condition in the case of no compensation. It is found that the input line current includes acute ripples around its peaks, of which main components are the fifth and the seventh as indicated in the FFT analysis result of Fig. 7 (b). A relative amount of these current harmonics with respect to the fundamental component is almost same as that of the simulation result. Fig. 8 demonstrates an experimental result with the proposed sixth-order harmonic active power suppression. As can be seen in the figure, the current ripples caused by the low-order harmonics are dramatically rejected and an appropriate sinusoidal current waveform is drawn by the PWMCSR.

Figs. 9 and 10 depict the total efficiency and the total input power factor, respectively. Striking difference in the total efficiency is not seen between with and without proposed technique, and the maximum efficiency is 88.5 % in both cases. However, the total input power factor is remarkably improved owing to the sixth-order harmonic active power suppression, especially in the lower-load range. This improvement is made mainly by the low-order harmonics rejection in the input line currents, which can be confirmed by the THD characteristics shown in Fig. 11. It is confirmed

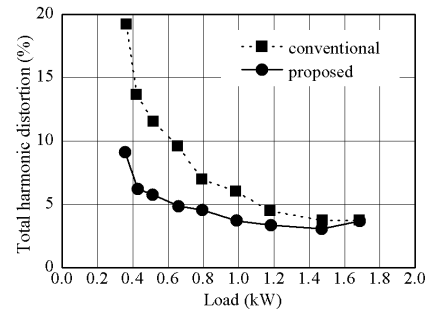


Fig. 11. Total harmonic distortion characteristics with/without sixth-order harmonic active power suppression (experimental result).

throughout the experimental tests that the average switching frequency of the PWMCSR is almost constant at 2 kHz over the full load range regardless of implementation of the compensation.

## VI. CONCLUSIONS

This paper described a technique to suppress a specific harmonic power in the DPC based PWMCSR. The proposed technique selectively reduces the specified order of the harmonic active power, which resultantly improves not only the input line current waveforms but also the total input power factor, especially in a low-load range. The performance of the proposed compensation technique was examined through computer simulations and experimental tests, and overall effectiveness was consequently confirmed by the operating waveforms, the total input power factor and the THD characteristics.

## REFERENCES

- [1] T. Ohnishi, "Three-Phase PWM Converter/Inverter by Means of Instantaneous Active and Reactive Power Control," *IEEE IECON Proc.*, vol. 1, 1991, p.p. 819-824.
- [2] T. Noguchi, H. Tomiki, S. Kondo, I. Takahashi and J. Katsumata, "Instantaneous Active and Reactive Power Control of PWM Converter by Using Switching Table," *IEE-Japan Trans. Ind. App.*, vol.116-D, no. 2, p.p. 222-223, 1996.
- [3] T. Noguchi, H. Tomiki, S. Kondo, and I. Takahashi, "Direct Power Control of PWM Converter Without Power-Source Voltage Sensors", *IEEE Trans. Ind. App.*, vol. 34, no. 3, 1998, p.p. 473-479.
- [4] M. Malinowski, M. Jesinski, and M. P. Kazmierkowski, "Simple Direct Power Control of Three-Phase PWM Rectifier Using Space-Vector Modulation (DPC-SVM)," *IEEE Trans. Ind. App.*, vol.51, no.2, 2004, p.p.447-454.
- [5] K. Toyama, O. Mizuno, T. Takeshita, and N. Matsui, "Suppression for Transient Oscillation of Input Voltage and Current-Source Three-Phase AC/DC PWM Converter", *IEEJ Trans. Ind. App.*, vol. 117-D, no. 4, 1997, p.p.420-426.
- [6] Y. Sato, T. Kataoka, "An Investigation of Waveform Distortion and Transient Oscillation of Input Current in Current Type PWM Rectifiers", *IEEJ Trans. Ind. App.*, vol. 114-D, no. 12, 1994, p.p.1249-1256.
- [7] Toshihiko Noguchi, Daisuke Takeuchi, Somei Nakatomi, and Akira Sato, "Novel Direct-Power-Control Strategy of Current-Source PWM Rectifier," *IEEE PEDS Proc.*, CDROM, 2005, p.p. 860-865.